



Thermally Triggered Drug Delivery by Polyhedral Oligomeric Silsesquioxane Co -Conjugated with Gold as a Nano-Drug Carrier in Cancer Therapy

Authors

Anusha Ponnusamy¹, Abiramee Ravi², Jaikumar V^{3*}, Kiruthiga Karunamoorthy⁴

¹Department of Microbiology, Thanjavur Medical College, Thanjavur (TN), India

²Sri Shakthi Institute of Engineering and Technology, Coimbatore (TN), India

^{3, 4*}Department of Chemical Engineering, Sri Sivasubramaniya Nadar College of Engineering, Chennai, India

Corresponding Author

Jaikumar V

Abstract

Nanoparticles can be modified with polymers and bioactive molecules aiming to achieve full efficiency in therapy and specific targeting. Polyhedral oligomeric silsesquioxane (POSS) is an organic-inorganic (RSiO_{1.5})₈ hybrid material that consists of a -Si-O- inorganic core surrounded by tunable organic moieties. POSS is a highly symmetrical, cage-like structure, possible to add functional groups, both organic and inorganic in precision. POSS has been synthesized and characterized using FT-IR, ¹H NMR, EDAX, SEM, and TEM. It has been developed along with the thiol end group and paves a space for cross-linked nanostructures formation POSS-SH. Voids and spaces in the POSS cross-linked nanocarrier give enough space for drug loading up to 50 weight percentages. Here the therapy is done with the help of drug delivery application in an acidic medium found in the cancer cell site and acts as an internal trigger for drug release from POSS. The Presence of thiol end terminal has a greater affinity for attachment of gold which in turn provides an add-on application of photo dynamic therapy this combination is gold POSS-SH-Au. Cell viability studies proved that the POSS nanostructures are biocompatible. The developed POSS nanostructures can even be activated at acidic conditions, used for sustained release of drugs at specific targets, and provide in-vivo stability until they reach the tumor site. The POSS-SH-Au resulted an improvement in aqueous stability as its chains have the tendency to wrap around the siloxane cage and prevent the water from getting close to the siloxane frameworks.

Keywords: POSS, Crosslinked POSS nanodrug carrier, Cancer drug delivery, Gold nanoparticles, Upconverting nanoparticles.

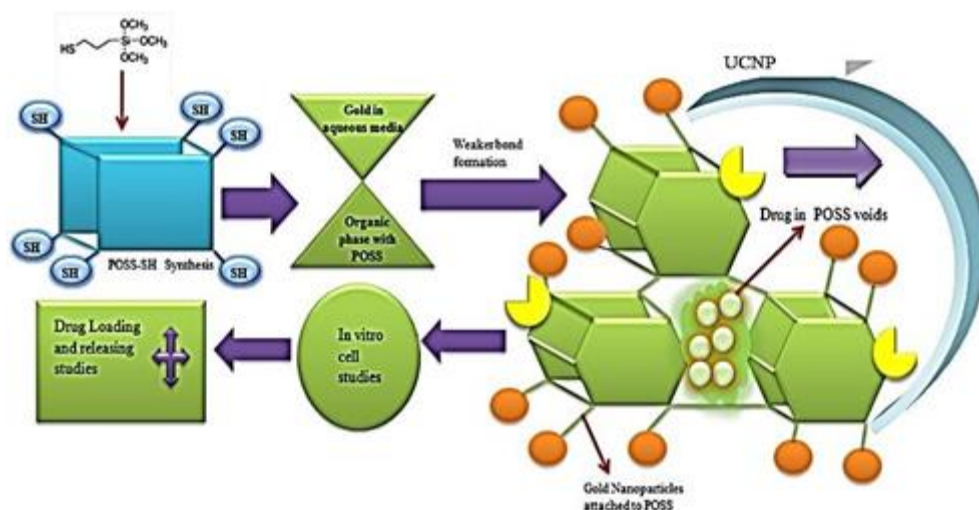


Figure 1. Pictorial representation of work

Introduction

Recently hybrid nanomaterials have gained a lot of attention owing to their notable properties such as hydrolytic stability, well-ordered structure, and high functionality active site frameworks. Hybrid compound of organic-inorganic silica-based frameworks have very high interaction with the polyfunctionalized materials^{1,3}. The interaction between the molecules is based on the functionalized silica nanomaterial synthesized with the structure directing agent. Multifunctional properties of hybrid nanomaterials focused on applications including drug delivery, desalination, theranostics, optical sensors and light emitting materials, etc². Different approaches have been used to synthesis a novel hybrid nanomaterial. The functional properties can be tailored accordingly in drug delivery applications⁶⁻⁷. Tailoring the functionality of hybrid materials will not affect the characteristics properties of the nanomaterials and it is the advantageous part utilized in nanoscience studies.

Cancer therapeutic treatments including chemotherapy, radiation therapy, photodynamic therapy, and anticancer drugs etc., causes serious side effects on healthy non-malignant cells⁴. A

targeted drug delivery is a prominent area of research in particularly the nanocarrier plays a key role in drug delivery. Folic acid has been used as a targeting ligand used in nanocarrier because most of the epithelial cancer cells over express folate receptors compared to the healthy non-cancerous cells⁸. Among various materials like Polymeric nanoparticles, Polymeric micelles, Liposomes, Dendrimers, Quantum dots, etc., used for developing drug carriers and the organic-inorganic nanohybrid polyhedral oligomeric silsesquioxane (POSS) carrier. POSS emerged as an efficient strategy in recent years due to its chemical inertness, biocompatibility and bioavailability properties. POSS is an organic-inorganic (RSiO_{1.5})₈ hybrid material which consists of an -Si-O- inorganic core surrounded by tunable organic moieties¹¹. It possesses attractive properties like high symmetry, smaller size (1-3 nm), thermal stability due to its rigidity, three-dimensionality, high mechanical strength, non-volatile and eco- friendly. It also acts as nanoscale enhancing agent in optical bioprobes in which it inhibits the aggregation of molecule thereby diminishing the effect of auto-quenching¹²⁻¹⁴.

Even though POSS holds unique physiochemical

properties, very little research has been carried out and more studies need to be done to find the cross-linked networks of POSS materials with large number of active terminal organic groups¹⁶. In the thiol terminated POSS, it is cross-linked using thiol linkages resulted in improved aqueous stability that is due to formation of cross bonds around the siloxane cage that prevents the water from getting close to the siloxane frameworks¹⁷. This hybrid POSS material exhibits low toxicity, longer degradation time, smaller in size which makes it easily deliverable to the target site through vascular pores and also has high drug incorporation stability.

The phenomenon of up conversion helps to excite a hybrid material at a particular wavelength of the NIR region and get emission at comparatively lower wavelength¹⁸. Up converting nanoparticles (UCNP) are a class of nanoparticles that can get excitation at a longer wavelength and emission at a relatively shorter wavelength. The present study deals on the synthesis of a suitable core nanoparticle for PDT that has up converting properties which favors deeper tissue penetration¹⁹⁻²³. Up converting nanoparticles, provide the higher potential for the success of PDT in treating deep tissue tumors. The nanoparticles were coated with POSS-SH-Au to attain a biocompatible layer²⁵. The nanoparticles were coated with POSS-SH-Au-mesoporous silica that can be used as vehicle/carrier molecule to deliver photosensitizers directly to the site of action.

To best of our knowledge and vast literature survey, this is the first-time report on the synthesis of nanostructured hybrid nanomaterial using thiol terminated polyhedral oligomeric silsesquioxane (POSS) crosslinked by thiol linkages. Synthesized material paves a way for linking a functional compound to end of linkages. Gold nanoparticles introduced to POSS with thiol

terminals. Stronger interaction with thiol traps gold nanomaterial and that forms POSS (POSS-SH-Au NP)²⁸⁻³⁰.

The synthesized organic-inorganic POSS nanohybrid characterized to reveal the synthesized nanostructure. In addition, the biocompatible POSS nanostructure coated in up converting nanoparticles where the anti-cancer drug (DOX) or any photosensitizer can be loaded as core material³²⁻²⁶. The confirmation of biocompatibility studied with POSS, up converting nanoparticles and POSS coated up converting nanoparticles. Cell viability studied on L929 cell lines and C6C12 cell lines with varied concentrations of each nanomaterial. The biocompatibility, encapsulation efficiency and cell viability were analyzed *in vitro*³⁹⁻⁴³. Nanostructured POSS could be useful as a possible carrier for anti-cancer drug delivery systems.

Materials and Method

Materials

(3-Mercaptopropyl) triethoxysilane (95%, MPTES) purchased from Alfa Aesar- Thermo Fisher, India. Toluene (99.0%), Dichloromethane (99.0%) and Hydrochloric acid (37-38%) purchased from EMPLURA, Mumbai- India. Gold (III) chloride trihydrate (99.0%) were purchased from HiMedia Laboratories, India. Ethanol was purchased from Changshu Yangyan Chemicals, China.

Carbinol (99.0%) was purchased from FINAR limited, India. Distilled water was used for all experiments. All the mentioned chemicals were used without any further purification. Cetyl trimethyl ammonium bromide (98%, CTAB), purchased from SPECTROCHEM PVT.LTD, Mumbai.

Sodium borohydride (95%, NaBH₄), purchased from Merck specialities pvt. Ltd, Mumbai.

Ethanol (99%), Purchased from Changshu Hongsheng Fine chemicals Co. Ltd. Aminopropyl triethoxysilane (APTES), Tetraethyl orthosilicate (TEOS), Hydrochloric acid (HCL), Erbium (III) chloride hexahydrate, Ytterbium (III) nitrate pentahydrate and Yttrium (III) nitrate hexahydrate were purchased from Sigma Aldrich. Ammonium fluoride (98%), toluene was purchased from Avra chemicals. Sodium Nitrate was purchased from Fischer Scientific. Pluronic-123 and Polyvinyl pyrrolidone (PVP) were purchased from Sigma aldrich and Sodium dodecyl sulphate Deionised was purchased from Himedia. Distil water was used for all experiments. Dulbecco's Phosphate buffer saline (500ml, PBS) Gibco by Life technologies corporation, Canada. Trysin-EDTA (IX, 0.05%) Life technologies corporation, Canada. Penicillin streptomycin (100ml) Gibco by Life Technologies Corporation, Canada. Cell titer 96 – Aqueous one solution Cell proliferation Assay, PROMEGA, USA. 96 Well culture cluster flat Bottom, Costar, Corning Incorporated, NY, USA.

Synthesis of POSS-SH nanoparticles

In a typical synthesis of thiol terminated POSS (POSS-SH), 10ml of (3-Mercaptopropyl) triethoxysilane was taken in 120ml of methanol (Carbinol)⁴⁻⁶. About 20ml of hydrochloric acid was added drop wise and then kept under reflux condition with Nitrogen atmosphere at 70° C for 36Hrs under constant stirring. The product was washed with refrigerated methanol for two times and with Dichloromethane for three times. The solvent was removed from the medium using vacuum drying method (rotavac)- 3 hrs. A white color gelatinous likePOSS-SH was obtained.

Synthesis of POSS-SH-Au Nanoparticles To obtain the Au terminated POSS, thiol terminated

POSS and organic media with toluene were taken in the ratio of 1:2, in theseparating funnel. 100mg of Gold source - Gold (III) chloride trihydrate along with the 0.185g of CTAB a cationic surfactant acting a bridging compound for crosslinking POSS-SH with gold¹¹⁻¹³. In 50ml distilled water which is in aqueous phase contains CTAB and Gold source holding in 100mL separating flask. In order to create a weakerforce of interaction between crosslink the media containing flask is shaken well for 1hr. The mixture was kept under constant stirring in 40°C for 3hrs. Then 0.01g of NaBH₄ added in the end of stirring. The moisture was removed from the medium using vacuumdrying method (rotavac)- 5 hrs. A white powdered precipitate like Au terminatedPOSS-SH was obtained.

Synthesis of up converting nanoparticles

NaYF₄ host doped with Er³⁺ and Yb³⁺ in ratios of 1:10, 0.5:10, 0.1:10 where 1, 0.5 and 0.01 denotes the concentration of the dopants (i.e Er³⁺ and Yb³⁺) in the host crystal NaYF₄. Surfactant of 10mg mixed in 5 ml water and NaNO₃ was added to make 1 molar solution. Y(NO₃)₃.6H₂O and Erbium Nitrate in 40 ml of water to make 1 molar solution with dopant concentration of 1%, 5% and 10%³¹⁻³³. Then Ammonium Fluoride (4 moles) in 5ml was added dropwise to sol C at 80°C, stirred for 2h and autoclave for 12 hours under 180°C and centrifuged and dried to get product. The concentration quenching is studied by varying the concentration of the dopant is the further course of work. For codoping we used NaYF₄: Yb³⁺: Er³⁺ in the ratio 78:20:2 for maximum upconversion efficiency.

Preparation of UCNPs coated with POSS-SH-Au

To obtain the POSS coated UCNP, organic phase with toluene POSS-SH, sourced with Au less than 100nm sized. Prepared UCNPs of 100mg added in the POSS-SH organic phase mixture¹⁵⁻

¹⁹. 0.185g of CTAB a cationic surfactant acting a bridging compound for crosslinking POSS-SH with gold. In 50ml distilled water which is in aqueous phase contains CTAB and Gold source holding in 100mL separating flask. In order to create a force of interaction between crosslink the media containing flask is shaken well for 1hr. The mixture was kept under constant stirring in 40°C for 3hrs. Then 0.01g of NaBH₄ added in the end of stirring. The moisture was removed from the medium using vacuum drying method (rotovac)- 5 hrs. A white colored powdered precipitate like UCNPs terminated POSS-SH-Au obtained.

Characterization techniques

The synthesized POSS-SH was characterized using Fourier transform-infrared spectroscopy (FT-IR, Spectrum 100, Perkin Elmer, USA), The morphology of the different sized NPs was measured using Field emission scanning electron microscope, Tescan. transmission electron microscopy (TEM, JSM2100F, JEOL, Japan), Proton magnetic resonance spectroscopy (¹H NMR, Bruker, Germany). The thermal stability of silica nanoparticles assisted Ca_{1-x}SiO₄:xEu³⁺ phosphors was recorded on a SDT Q600, TG analyser³².

Cell Culture

L929 and C2C12 cell line was obtained from CeNTAB Culture Collection. Cells were grown in RPMI medium with fetal bovine serum (FBS) 10% and incubated at 37 °C, 5% CO₂ in a humidified incubator. The growth of cells seen in 2x10⁶ cells/ml and subcultured when confluence reached 60- 70% every 2-3 days.

Toxicity Assays

Both L929 and C2C12 cells were seeded at 10,000 cells/well in a 96-flat plate then

incubated for 18 hours to allow adherence. Nanoparticles (UCNPs, POSS-SH-Au and UCNPs+POSS-SH-Au)²²⁻²³ were diluted in fresh medium. After incubation, cells were treated with five Nanoparticles range between (0.001-100mg/mL) for 1, 24 and 48h. The solution was removed, and the cells were washed twice with phosphate buffered saline (PBS) twice to remove excess nanoparticle residue.

3-(4,5-Dimethylthiazol-2-yl)-2,5-Diphenyltetrazolium Bromide (MTT) Assay Experimental Procedure

The toxicity of POSS-SH-Au, UCNPs and UCNPs+POSS-SH-Au nanoparticles determined by MTT assay²⁰⁻²⁶. 1x10⁴ cells were seeded in volume of 100 µl into 96-well flat bottom plate. MTT was added to each well at 0.5 mg/mL, and then plates were incubated at 37 °C for 4h, then 80 µl of 20% SDS in 0.02 M HCl was added to each well. The plates were kept in the dark at room temperature for overnight. OD was read on ELISA reader at 570 nm, with 630 nm as reference wavelength.

Results and Discussions

FT-IR characterization of POSS-SH

The FT-IR spectrum of POSS-SH are shown in Figure 1. The FT-IR spectra of Thiol terminated POSS showed bands at 1100 cm⁻¹ which is corresponding to -SH bending, respectively. This confirms the thiol functionalization of POSS. The propyl group of thiols in the thiol terminated POSS are revealed by the -CH₂- stretching vibrations located at 2916-2936 cm⁻¹. The band at 1704 cm⁻¹ represents the presence of carbonyl groups on the cross-linked POSS nanostructures. The peak at 1100 cm⁻¹ indicates the presence of Si-O-Si bond thereby confirms the formation of POSS. Likewise, in the study conducted by⁴² there observed approximately similar spectral peaks shows the presence of the

typical bands of vinyl-POSS molecule, such as the band at 1604 cm^{-1} corresponding to the C=C stretching vibration of the vinyl group. The bands at 2960 and 3066 cm^{-1} are attributed to the unsaturated =C-H symmetric and asymmetric stretching vibration respectively. In addition, the bands at 1410 and 1946 cm^{-1} are assigned to the scissor bending vibration and overtones absorption of ethylene end groups. It was observed that wide band at 1125 cm^{-1} and narrow band at 780 cm^{-1} are associated with the Si-O-Si and Si-C stretching vibrations of the POSS monomer respectively.

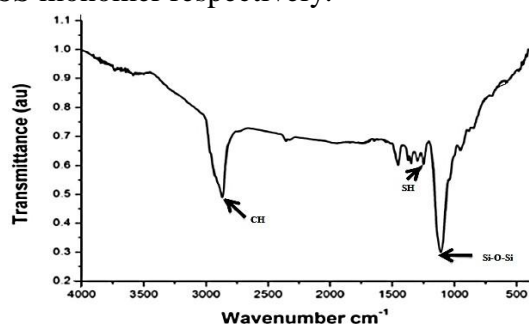


Figure 2 FTIR characterization of POSS-SH

signals were observed, indicative of degradation of the vinyl bond during synthesis. For samples prepared from mixtures of the precursors, (VTES/TEOS) signals related to the vinyl proton at between 5.88 and 6.2 ppm also observed. All POSS samples synthesized, independent of the method used, showed a signal at 3.5–3.8 ppm, suggesting the presence of silanol without condensation⁴³.

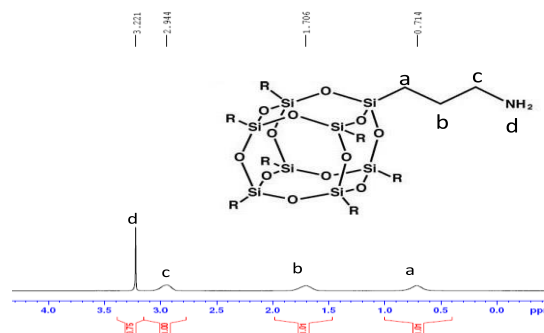


Figure 2. ¹H NMR characterization of POSS-SH

Table 1. FT-IR shows functional groups present in POSS-SH

Wavenumber (cm ⁻¹)	Corresponding vibrations
2916-2936	-CH ₂ - stretching
1000	Si-C stretching
1100	-Si-O-Si- stretching
1704	Carboxylic groups

NMR characterization POSS-SH

Figure 2. shows the proton NMR of POSS- SH. The peak at δ 0.71 ppm confirms the proton attached to the POSS units and the peaks at δ 1.70 ppm and δ 2.94 ppm confirm the organic terminal moieties -CH₂-CH₂- attached with POSS. The peak at δ 3.22-ppm represents the proton attached to the amine thereby confirms the thiol terminated POSS formation (POSS-SH). At 1.61 and 2.2-ppm methylene, proton

Morphological studies of POSS-SH

The external morphologies were determined by using SEM analysis. The SEM images show the size of thiol terminated POSS which is about 100 nm. SEM images in various magnifications shows the cage shape of POSS-SH and clear voids in between each cage are visible.

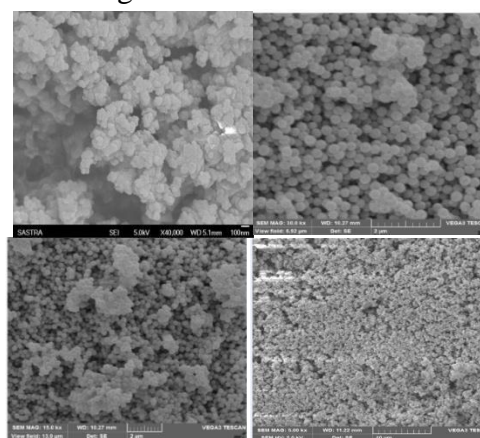


Figure 3. SEM images of POSS-SH. Morphological studies of POSS-SH-Au

The internal morphology of POSS-SH-Au is examining using TEM images. The size after

crosslinking the POSS units into POSS-SH- Au nanostructures were found to be 200nm which is observed from transmission electron microscopic images. TEM image provided the result of gold present in the terminals of each POSS-SH. This confirmation ensures the gold nanoparticles surrounded POSS-SH with the strong force of attraction between them. Moreover, in a similar fashion on another study morphology of the micrographs of the POSS synthesized with VTES via dielectric heating, where the formation of irregular cubic clusters of submicron order, with an average size of around 0.88 μm , observed. This morphology been observed in studies related to polymer nanocomposites using VTES as the precursor.⁴⁴

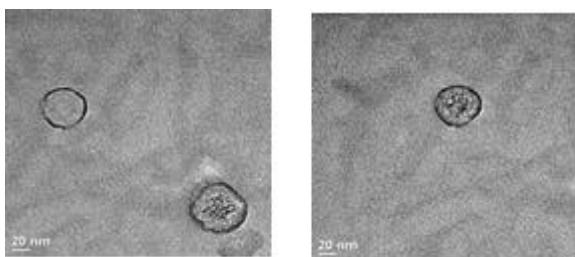


Figure 4. TEM image of POSS-SH-Au

3.5. Chemical composition of POSS-SH-Au

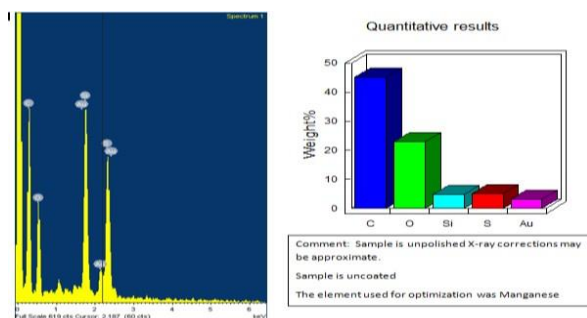


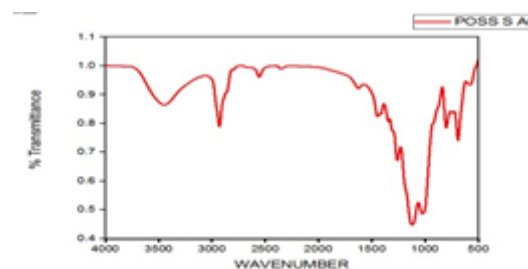
Figure 5. EDAX for POSS-SH-Au

Chemical composition analysis is further confirmed by (EDAX) Energy dispersive X-Ray spectroscopy. Figure 5 shows the uncoated POSS-SH-Au provides the presence of carbon,

oxygen, silica, Sulphur, and gold in various proportionalities. An uncoated sample shows the presence of Au content in the compositional result. Each POSS units have less than 10% gold in its surface.

FTIR characterization for POSS-SH-Au

The FT-IR spectrum of POSS-SH-Au are shown in Figure 6. The FT-IR spectra of Au terminated POSS-SH showed bands at 1100cm^{-1} which are corresponding to -SH bending, respectively. This confirms the thiol functionalization of POSS. The propyl group of thiols in the thiol terminated POSS are revealed by the -CH₂- stretching vibrations located at $2922\text{-}2937\text{ cm}^{-1}$. The band at 1725 cm^{-1} represents the presence of carbonyl groups on the cross-linked POSS nanostructures.



The peak at 1000 cm^{-1}

Figure 6. FTIR characterization of POSS-SH-Au

Table 2. FTIR- POSS-SH-Au

Wave number (cm ⁻¹)	Corresponding vibrations
2922 - 2937	-CH ₂ - stretching
1100	-SH stretching
1000	-Si-O-Si- stretching
1725	Carboxylic groups

NMR Characterization of POSS-SH-Au

In Figure 7. shows the proton NMR of POSS-SH-Au. The peak at δ 061 ppm confirms the proton attached to the POSS units and the peaks at δ 1.52

ppm and δ 2.554 ppm confirm the organic terminal moieties -CH₂-CH₂- attached with POSS.

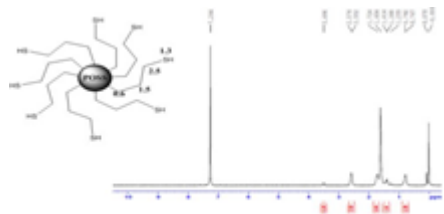


Figure 7 Proton NMR for POSS-SH-Au dried sample

The peak at δ 1.32 ppm represents the proton attached to the amine thereby confirms the thiol terminated POSS formation (POSS-SH-Au).

Thermal stability analysis – Thermo Gravimetric analysis study

Thermo-gravimetry analysis of POSS-SH sample has been done to understand the thermal stability of synthesized POSS-SH molecule. Figure 8 shows the thermos-gravimetric pattern of POSS-SH. The experiment was performed from room temperature to 900°C with the rate of 10°C/min. The result shows change in weight of POSS-SH at four different temperatures. The temperature at about 100-200°C, there is a loss of 14% recorded which may be due to the evaporation of moisture from the sample.

Nano composites were lower than neat polyimide. This may be due to the low molecular weight of the PI-POSS, which was caused by the unequal amounts of diamine and dianhydride added in these systems. The residual char yields after the incorporation of 0, 5, 10 and 15 wt.% POSS cube into the PI were 43.4, 47.6, 48.8 and 50.4% respectively, at 900°C and this indicated that these hybrid materials were thermally stable.

SEM and TEM analysis of UCNP

The scanning electron microscope image shown in Figure 9. (a) depicts the UCNP coated with mesoporous-silica with a monodisperse size range of 100nm. Thus the obtained size range is in the

optimal size of the UCNP needed for biological application. The transmission electron microscope image shown in figure 9. (b) depicts the UCNP coated with mesoporous-silica in the desired core-shell structure

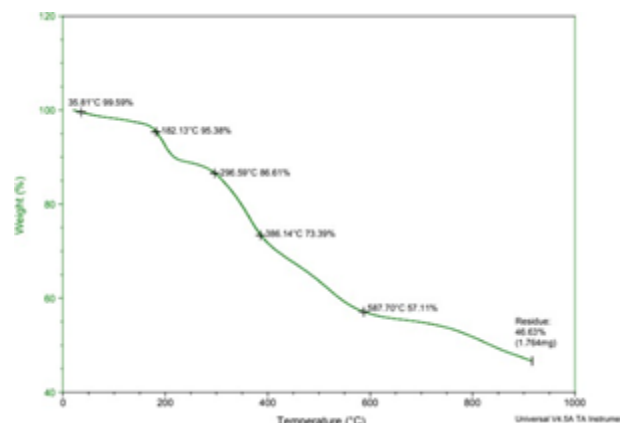


Figure 8. TGA for POSS-SH-Au dried sample

Above 200°C of temperature, there are three different steps found such as the loss of 13% at 300-400°C, loss of 17% at 500-600°C and a loss of 9-10% at high temperature above 600°C. These are corresponding to the loss of thermally unstable organic molecules present along with POSS molecule. Finally, 46% of the sample is left as residue which indicates the formation of SiO₂ at high temperature. Overall, the loss of only 5% until 200°C shows the good thermal stability of synthesized POSS-SH nanoparticles. In a similar study⁴⁵ POSS-PI (POSS-Polyimide) nanocomposites was prepared and was subjected to TGA analysis. In that thermogram, the initial degradation temperatures for the POSS-PI

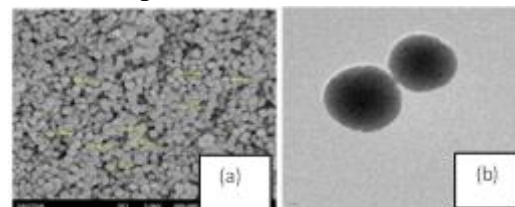


Figure 9. (a) SEM image showing outer morphology of UCNP, (b) TEM image showing core-shell structure of UCNP coated with mesoporous silica.

In vitro cell viability studies

The cytotoxicity of POSS-SH-Au assessed by MTS assay. Along with it cytotoxicity of prepared UCNPs and POSS-SH-Au coated on UCNP assessed by MTS assay. Cell viabilities were carried out using mouse fibroblast cell line (L929) and mouse myoblast cell line (C2C12). The cells were counted using a hemocytometer and 1000 cells were seeded in each well of the 96 well plate and was let to adhere for 12h. After 12h, the dose of the 3 materials (UCNP, POSS, UCNP+POSS) was added to bathes containing 5 wells each and the concentrations added being 5, 10, 25, 50, 100 and 200 microgram/microlitre each and incubated at 37°C for 24h. After 24h of incubation the 96 were removed from the incubator, the used-up media from the wells were removed and the wells were washed with 200 microlitres of PBS at a pH of 7.4 and then 200 microlitres of serum free media was added along with 50 microlitres of MTS solution. The unreacted MTS was removed and the optical density at various concentrations of POSS-SH-Au was measured using microplate reader which kept in incubator for 2 hours. Absorbance is calculated at 490nm using well plate reader. Thus, we can conclude that higher the absorbance value the more the number of viable cells in the well. Figure 10 shows the cell-viability studies of POSS-SH-Au, UCNPs and POSS-SH-Au coated on UCNP. The result shows the 86% viability of cells at higher concentration of 200 µg/ml. So, it proves that the POSS based molecules are highly bio-compatible which can help to use it as therapeutic tool. Also shows compatibility at higher rates in POSS-SH-Au coated on UCNP. In a similar study happened on POSS & Au of the 8 NPs examined for potential interference with the components of the MTT assay, the presence of trisilanolphenyl POSS and trisilanol isoctyl POSS resulted in a significant alteration in MTT standard curve. There were decrease in ODs for ≥ 10,000 cells/well when the particles were

added with either the MTT or the SDS. These changes were significant (P 0.05). As observed, there were smaller no significant changes for ethanol and trisilanol cyclopentyl POSS when added with SDS in MTT.⁴⁵

$$\text{Cell viability (\%)} = \left(\frac{\text{Average optical density of POSS-SH-Au groups}}{\text{Average optical density of control groups}} \right) * 100$$

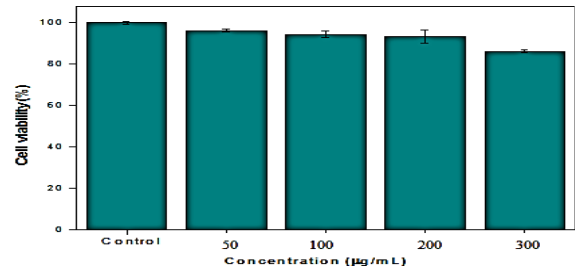


Figure 10. Cell-viability studies–MTS Assay. Shows 78% biocompatibility of POSS-SH-Au

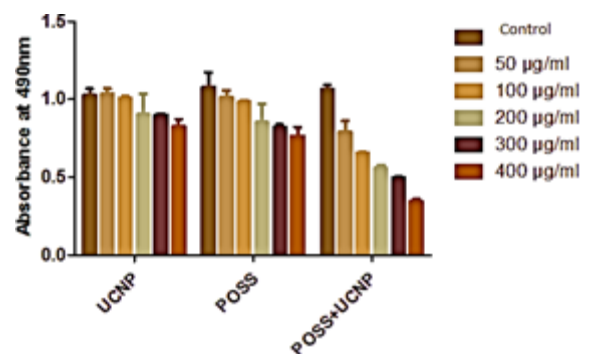


Figure 11. Cell viability studies in L929 cell line – MTS assay for different concentrations

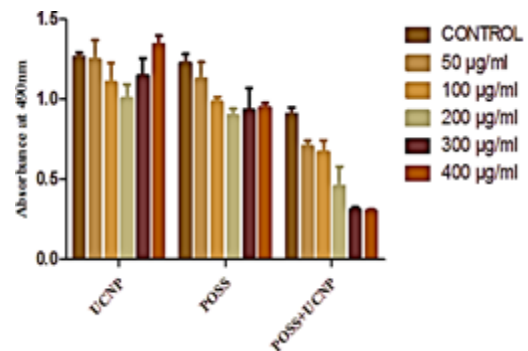


Figure 12. Cell viability studies in C2C12 cell line – MTS assay for different concentrations.

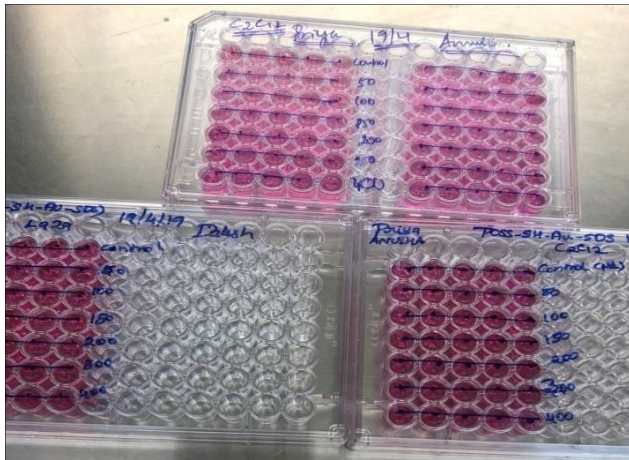


Figure 13. Cell viability testing – (96 well plate) Cell seeding procedure in biosafety cabinet.

From figure 14 shows that when the mouse myoblast cells were made to interact with POSS, till the concentration of 200 $\mu\text{g}/\mu\text{l}$, evident toxicity was not observed in the cells was observed when the concentration of POSS was observed above 300 $\mu\text{g}/\mu\text{l}$. This has been ascertained by the graph in figure 12 which depicts the MTS assay. The cells tend to move towards corners of the well as they tend to avoid contact with the material.

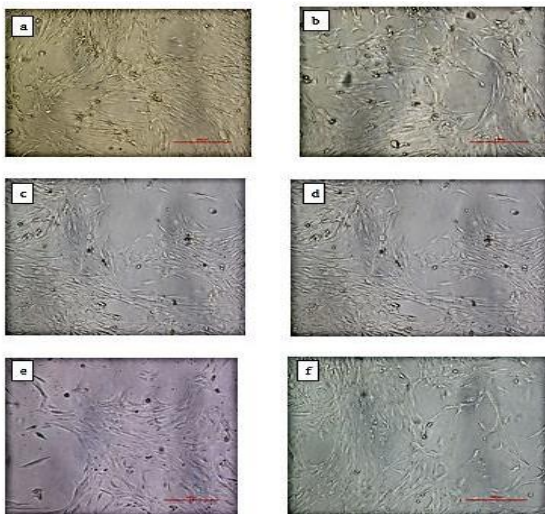


Figure 14. MTS Assay in C2C12 cell line with POSS-SH-Au nanocarrier (a) Control (b) 50 $\mu\text{g}/\text{ml}$ (c) 100 $\mu\text{g}/\text{ml}$ (d) 200 $\mu\text{g}/\text{ml}$ (e) 300 $\mu\text{g}/\text{ml}$ (f) 400 $\mu\text{g}/\text{ml}$

From figure 15 shows that when the mouse myoblast cells were made to interact with UCNPs, till the concentration of 200 $\mu\text{g}/\mu\text{l}$, no evident toxicity was not observed in the cells. This has been ascertained by the graph in figure 12 which depicts the MTS assay. The cells do not tend to move towards corners of the well to avoid contact with the material and they can be seen freely interacting with the material at all concentrations. No major difference in the morphology is seen in the cells.

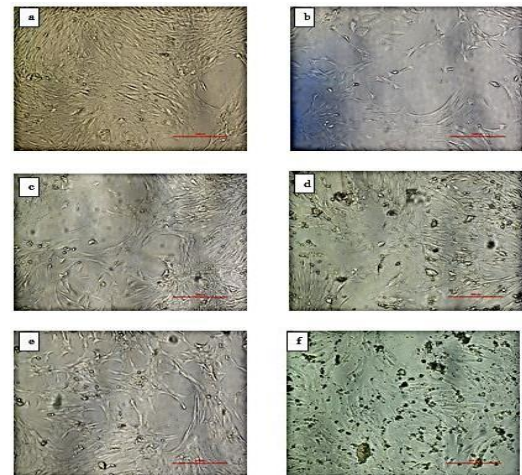


Figure 15. MTS Assay in C2C12 cell line with UCNPs (a) Control (b) 50 $\mu\text{g}/\text{ml}$ (c) 100 $\mu\text{g}/\text{ml}$ (d) 200 $\mu\text{g}/\text{ml}$ (e) 300 $\mu\text{g}/\text{ml}$ (f) 400 $\mu\text{g}/\text{ml}$

From figure 16 shows that when the mouse myoblast cells were made to interact with POSS + UCNPs, till the concentration of 25 $\mu\text{g}/\mu\text{l}$, evident toxicity was not observed in the cells was observed when the concentration of the material was observed above 50 $\mu\text{g}/\mu\text{l}$, this has been ascertained by the graph in figure 12 which depicts the MTS assay. The cells tend to move towards corners of the well as they tend to avoid contact with the material. The cells do not show any change in morphology.

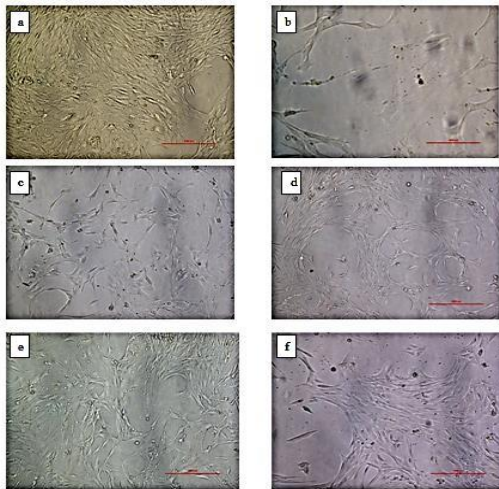


Figure 16. MTS Assay in C2C12 cell line with POSS-SH-Au coated with UCNP nanocarrier (a) Control (b)5 µg/ml (c)10 µg/ml (d)25 µg/ml (e)50 µg/ml (f)100 µg/ml

From figure 17 shows that when the mouse fibroblast cells were made to interact with POSS, till the concentration of 200 µg/µl, evident toxicity was not observed in the cells was observed when the concentration of POSS was observed above 300 µg/µl, this has been ascertained by the graph in figure 11 which depicts the MTS assay. The cells tend to move towards corners of the well as they tend to avoid contact with the material.

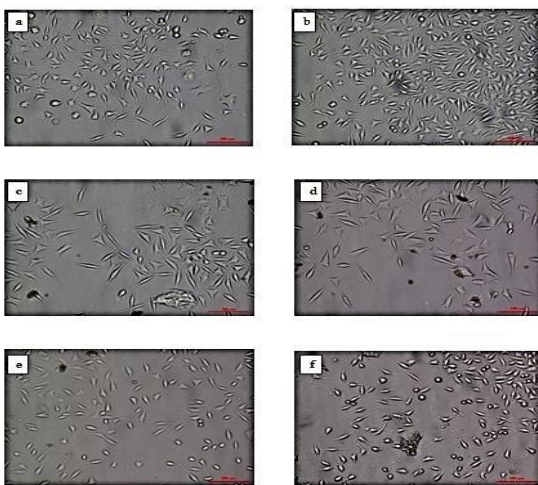


Figure 17. MTS Assay in L929 cell line with POSS-SH-Au (a) Control (b)50 µg/ml (c)100 µg/ml (d)200 µg/ml (e)300 µg/ml (f)400 µg/ml

From figure 18 we can find that when the mouse fibroblast cells were made to interact with UCNP, till the concentration of 200 µg/µl, no evident toxicity was not observed in the cells. This has been ascertained by the graph in figure 11 which depicts the MTS assay. The cells do not tend to move towards corners of the well to avoid contact with the material and they can be seen freely interacting with the material at all concentrations. No major difference in the morphology is seen in the cells.

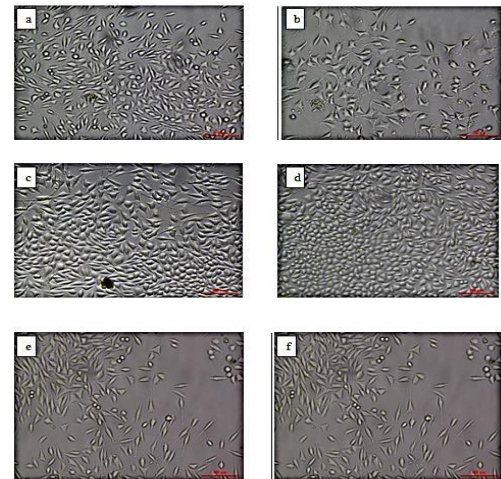


Figure 18. MTS Assay in L929 cell line with UCNPs (a) Control (b)50 µg/ml (c)100 µg/ml (d)200 µg/ml (e)300 µg/ml (f)400 µg/ml

From figure 19 we can find that when the mouse fibroblast cells were made to interact with POSS + UCNP, till the concentration of 25 µg/µl, evident toxicity was not observed in the cells was observed when the concentration of the material was observed above 50 µg/µl, this has been ascertained by the graph in figure 11 which depicts the MTS assay. The cells tend to move towards corners of the well as they tend to avoid contact with the material. The cells do not show any change in morphology.

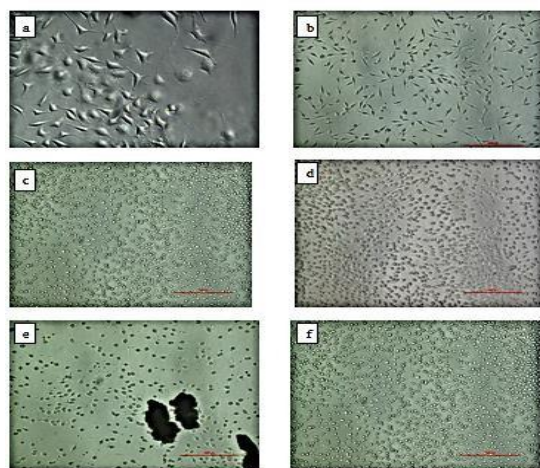


Figure 19. MTS Assay in L929 cell line with UCNP coated POSS-SH-Au (a) Control (b)5 µg/ml (c)10 µg/ml (d)25 µg/ml (e)50 µg/ml (f)100 µg/ml

Conclusions and Future Prospects

In this work, thiol terminated POSS has been synthesized successfully which is then modified using gold nanoparticles to crosslink the POSS molecules by thiol linkage. The materials were characterized using various techniques. The carrier of drug is examined for its biocompatibility in two cell lines (C2C12 and L929). In order to improve the biocompatibility of the carrier the POSS-SH-Au attached with up converting nanoparticles also showed biocompatibility in MTS assay test. The POSS-SH-Au carrier of smaller dimension can be used as a drug delivery vehicle for cancer therapy which provides excellent biocompatibility and also site-specific targeting to the malignant cells. Targeted drug release can be achieved by using folic acid receptors as it is over expressed in the cancer cells. This can even be activated at acidic conditions as the rigid frameworks of the POSS provide *In vivo* stability. As the size of the POSS nanocarriers is small, it possesses efficient uptake, and it will be degraded into non-toxic small molecules such as diacids, silica which can be easily excreted from the body.

Conflict of interest

Conflict of interest declared none

Reference

1. Ahmad Mehdi, Catherine Reye, Robert Corriu, From molecular chemistry to hybrid nanomaterials. Design and functionalization. *Journal of chemical society reviews*, 2; 2011.
2. Clement Sanchez, Philippe Belleville, Michael Popall, Lionel Nicole, Applications of advanced hybrid organic-inorganic nanomaterials: from laboratory to market, *Journal of Chemical Society Reviews*, 2, 2011.
3. Xin Du, Bingyang Shi, Ji Liang, Jingxu Bi, Sheng Dai, Shi Zhang Qiao, Developing Functionalized Dendrimer-Like Silica Nanoparticles with Hierarchical Pores as Advanced Delivery Nanocarriers, 25, 2013; 5981-5985.
4. Takuya Iwamoto, Clinical application of drug delivery systems in cancer chemotherapy: review of the efficacy and side effects of approved drugs, *Biological and Pharmaceutical Bulletin*, 5, 2013.
5. Nair, B. P., Vaikkath, D., & Nair, P. D. (2013). Polyhedral oligomeric silsesquioxane-F68 hybrid vesicles for folate receptor targeted anti-cancer drug delivery. *Langmuir*, 30(1), 340-347
6. Tanaka K, Jeon J H, Inafuku, K, and Chujo Y (2012) Enhancement of optical properties of dyes for bioprobes by freezing effect of molecular motion using POSS-core dendrimers. *Bioorganic & medicinal chemistry*, 20(2), 915-919.
7. Zhou H, Ye Q, and Xu J (2017) Polyhedral oligomeric silsesquioxane-based hybrid materials and their applications. *Materials Chemistry Frontiers*, 1(2), 212-230.

8. Surface Modification of Gold Nanoparticles with Polyhedral Oligomeric Silsesquioxane and Incorporation within Polymer Matrices Shiao-Wei Kuo, Yung-Chien Wu, Chu-Hua Lu, Feng-Chih Chang, Wiley InterScience, DOI: 10.1002/polb.21686
9. Phillips S H, Haddad T S, and Tomczak S J (2004) Developments in nanoscience: polyhedral oligomeric silsesquioxane (POSS)-polymers. *Current Opinion in Solid State and Materials Science*, 8(1), 21-29.
10. McCusker C, Carroll J B and Rotello V M (2005) Cationic polyhedral oligomeric silsesquioxane (POSS) units as carriers for drug delivery processes. *Chemical Communications*, (8), 996-998.
11. Chen K B, Chang Y P, Yang S H, and Hsu C S (2006) Novel dendritic light-emitting materials containing polyhedral oligomeric silsesquioxanes core. *Thin Solid Films*, 514(1-2), 103-109.
12. Sheikh F A, Barakat N A, Kim B S, Aryal S, Khil M S, and Kim H Y (2009) Self-assembled amphiphilic polyhedral oligosilsesquioxane (POSS) grafted poly(vinyl alcohol) (PVA) nanoparticles. *Materials Science and Engineering: C*, 29(3), 869-876.
13. Kim K O, Kim B S, and Kim, I S (2011) Self-Assembled Core-Shell Poly (Ethylene Glycol)-POSS Nanocarriers for Drug Delivery. *Journal of Biomaterials and Nanobiotechnology*, 2(3), 201-206.
14. Pu Y, Chang S, Yuan H, Wang G, He B, and Gu Z (2013) The anti-tumor efficiency of poly (L-glutamic acid) dendrimers with polyhedral oligomeric silsesquioxane cores. *Biomaterials*, 34(14), 3658-3666.
15. Yang, Y. Y., Wang, X., Hu, Y., Hu, H., Wu, D. C., & Xu, F. J. (2013) Bioreducible POSS-cored star-shaped polycation for efficient gene delivery. *ACS applied materials & interfaces*, 6(2), 1044-1052.
16. Gandhi S, Kumar P, Thandavan K, Jang K, Shin D S, and Vinu A (2014) Synthesis of a novel hierarchical mesoporous organic-inorganic nanohybrid using polyhedral oligomeric silsesquioxane bricks. *New Journal of Chemistry*, 38(7), 2766-2769.
17. Wang X, Yang Y, Gao P, Li D, Yang F, Shen H and Wu D (2014) POSS dendrimers constructed from a 1→7 branching monomer. *Chemical communications*, 50(46), 6126-6129.
18. Teng C P, Mya K Y, Win K Y, Yeo C C, Low M, He C, and Han M Y (2014) Star-shaped polyhedral oligomeric silsesquioxane-polycaprolactone-polyurethane as biomaterials for tissue engineering application. *NPG Asia Materials*, 6(11), e142.
19. Abdulmajeed Almutary, (2017) Toxicity of four novel Polyhedral Oligomeric Silsesquioxane (POSS) particles used in anti-cancer drug delivery. *Journal of Applied Pharmaceutical Science* Vol. 7 (02), pp. 101-105.
20. Mosmann T., Rapid colorimetric assay for cellular growth and survival: application to proliferation and cytotoxicity assays. *Journal of immunological methods*, 1983; 65, 55-63
21. Salata O. V, Applications of nanoparticles in biology and medicine. *Journal of nanobiotechnology*, 2004; 2, 1.
22. Neyertz S, Brown D, Pilz M, Rival N, Arstad B, Mannle F, and Simon C (2015) The stability of amino-functionalized polyhedral oligomeric silsesquioxanes in water. *The Journal of Physical Chemistry*

- B*, 119(21), 6433-6447.
23. Piorecka K, Radzikowska E, Kurjata J, RozgaWijas K, Stanczyk W A, and Wielgus E (2016) Synthesis of the first POSS cage–anthracycline conjugates via amide bonds. *New Journal of Chemistry*, 40(7), 5997-6000.
 24. Q Li, L Sun, W Zhou Z and Huang Y (2016) Dual stimuli-responsive hybrid polymeric nanoparticles self-assembled from POSS-based starlike copolymer-drug conjugates for efficient intracellular delivery of hydrophobic drugs. *ACS applied materials & interfaces*, 8(21), 13251-13261.
 25. Pramudya I, Rico C G, Lee C, and Chung H (2016) POSS-containing bioinspired adhesives with enhanced mechanical and optical properties for biomedical applications. *Biomacromolecules*, 17(12), 3853-3861.
 26. Narikiyo H, Kakuta T, Matsuyama H, Gon M, Tanaka K, and Chujo Y (2017) Development of the optical sensor for discriminating isomers of fatty acids based on emissive network polymers composed of polyhedral oligomeric silsesquioxane. *Bioorganic & medicinal chemistry*, 25(13), 3431-3436.
 27. Zhou H, Ye Q, and Xu J (2017) Polyhedral oligomeric silsesquioxane-based hybrid materials and their applications. *Materials Chemistry Frontiers*, 1(2), 212-230.
 28. Sha Ding, Yuejun Liu and Zhengjian Qi (June 2017) Facile Synthesis and Self-Assembly of Amphiphilic Polyether-Octafunctionalized Polyhedral Oligomeric Silsesquioxane via Thiol-Ene Click Reaction. *Polymers* 2017, 9, 251; doi:10.3390/polym907025.
 29. Yung-Chien Wu, Chu-Hua Lu, Feng-Chih Chang (February 2009) Surface Modification of Gold Nanoparticles with Polyhedral Oligomeric Silsesquioxane and Incorporation within Polymer Matrices. *Polymer Physics, Vol. 47, 811–819 (2009) VVC 2009 Wiley Periodicals, Inc.*
 30. Idris, N. M., Gnanasammandhan, M. K., Zhang, J., Ho, P. C., Mahendran, R., & Zhang, Y. (2012). In vivo photodynamic therapy using upconversion nanoparticles as remote- controlled nanotransducers. *Nature medicine*, 18(10), 1580.
 31. Tian, G., Ren, W., Yan, L., Jian, S., Gu, Z., Zhou, L., ... & Zhao, Y. (2013). Red-Emitting Upconverting Nanoparticles for Photodynamic Therapy in Cancer Cells Under Near-Infrared Excitation. *Small*, 9(11), 1929-1938.
 32. Wen, H., Zhu, H., Chen, X., Hung, T. F., Wang, B., Zhu, G., & Wang, F. (2013). Upconverting near-infrared light through energy management in core–shell–shell nanoparticles. *Angewandte Chemie International Edition*, 52(50), 13419-13423.
 33. Chen, G., Ohulchanskyy, T. Y., Kumar, R., Ågren, H., & Prasad, P. N. (2010). Ultrasmall monodisperse NaYF₄: Yb³⁺/Tm³⁺ nanocrystals with enhanced near-infrared to near-infrared upconversion photoluminescence. *ACS nano*, 4(6), 3163-3168.
 34. Dai, Y., Xiao, H., Liu, J., Yuan, Q., Ma, P. A., Yang, D., & Lin, J. (2013). In vivo multimodality imaging and cancer therapy by near-infrared light-triggered transplatinum pro-drug-conjugated upconversion nanoparticles. *Journal of the American Chemical Society*, 135(50), 18920-18929.
 35. Neyertz Brown D, Pilz M, Rival N, Arstad

- B, Mannle F, and Simon C(2015) The stability of amino-functionalized polyhedral oligomeric silsesquioxanes in water. *The Journal of Physical Chemistry B*, 119(21), 6433-6447.
36. Piorecka K, Radzikowska E, Kurjata J, RozgaWijas K, Stanczyk W A, and Wielgus E (2016) Synthesis of the first POSS cage-anthracycline conjugates via amide bonds. *New Journal of Chemistry*, 40(7), 5997-6000.
37. Q Li, L Sun, W Zhou Z and Huang Y (2016) Dual stimuli-responsive hybrid polymeric nanoparticles self-assembled from POSS-based starlike copolymer-drug conjugates for efficient intracellular delivery of hydrophobic drugs. *ACS applied materials & interfaces*, 8(21), 13251-13261.
38. Pramudya I, Rico C G, Lee C, and Chung H (2016) POSS-containing bioinspired adhesives with enhanced mechanical and optical properties for biomedical applications. *Biomacromolecules*, 17(12), 3853-3861.
39. Narikiyo H, Kakuta T, Matsuyama H, Gon M, Tanaka K, and Chujo Y(2017) Development of the optical sensor for discriminating isomers of fatty acids based on emissive network polymers composed of polyhedral oligomeric silsesquioxane. *Bioorganic & medicinal chemistry*, 25(13), 3431-3436.
40. Abiramee Ravi, Anusha Ponnusamy, Kirthika Krishnamoorthy, (2021) Preparation, Characterisation, *In-Vitro* Drug release and kinetics studies of Canaglifozin Polymeric nanoparticles, *Journal of Medical science and clinical research JMSCR*, 09, 06, Page 183-192.
41. Zhou H, Ye Q, and Xu J (2017) Polyhedral oligomeric silsesquioxane-based hybrid materials and their applications. *Materials Chemistry Frontiers*, 1(2), 212-230.
42. Xue, Meng & Zhang, Xian & Wu, Zhaofeng & Wang, Huan & Ding, Xin & Tian, Xingyou. (2013). Preparation and Flame Retardancy of Polyurethane/POSS Nanocomposites. *Chinese Journal of Chemical Physics*. 26. 445-450. 10.1063/1674-0068/26/04/445-450.
43. A. Beganskienė, V. Sirutkaitis, M. Kurtinaitienė, R. Juškėnas, A. Kareiva, FTIR, TEM and NMR investigations of Stöber silica nanoparticles, *Mater. Sci. (Medžiagotyra)* 10 (2004) 287–290.
44. B. Yang, H. Xu, J. Wang, S. Gang, C. Li, Preparation and thermal property of hybrid nanocomposites by free radical copolymerization of styrene with octavinyl polyhedral oligomeric silsesquioxane, *J. Appl. Polym. Sci.* 106 (2007) 320–3.
45. Almutary, A., & Sanderson, B. J. S. (2016). The MTT and Crystal Violet Assays. *International Journal of Toxicology*, 35(4), 454–462. Doi:10.1177/1091581816648906